Strong Binding of Noble Gases to $[B_{12}X_{11}]^-$: a theoretical study

Dedicated to Alexander I. Boldyrev on the occasion of his 70th birthday

Kevin Wöhner,[1,2,3] Toshiki Wulf,[1,3] Nina Vankova,[2] Thomas Heine[1,2,4]*

[1] Helmholtz-Zentrum Dresden-Rossendorf, Institute of Resource Ecology, Research Site Leipzig, 04318 Leipzig, Germany

[2] Faculty of Chemistry and Food Chemistry, School of Science, TU Dresden, 01062 Dresden, Germany

[3] Wilhelm Ostwald Institute of Physical and Theoretical Chemistry, Faculty for Chemistry and Mineralogy, Leipzig University, 04103 Leipzig, Germany

[4] Department of Chemistry, Yonsei University, Seodaemun-gu, Seoul 120-749, Republic of Korea

* *e-mail: thomas.heine@tu-dresden.de*

ABSTRACT We systematically explore the stability and properties of $[B_{12}X_{11}Ng]^-$ adducts resulting from the capture reaction of noble gas atoms (Ng) by anionic $[B_{12}X_{11}]^-$ clusters in the ion trap. $[B_{12}X_{11}]^-$ can be obtained by stripping one X^- ligand off the icosahedral *closo*-dodecaborate dianion $[B_{12}X_{12}]^{2-}$. We study the binding of the noble gas atoms He, Ne, Kr, Ar and Xe to $[B_{12}X_{11}]^-$ with ligands X = F, Cl, Br, I, CN. While He cannot be captured by these clusters and Ne only binds at low temperatures, the complexes with the heavier Kr, Ar and Xe show appreciable complexation energies and exceed 1 eV at room temperature in the case of $[B_{12}(CN)_{11}Xe]^-$. For the latter three noble gases, we observe a significant charge transfer from the Ng to the icosahedral B_{12} cage.

INTRODUCTION Boron, the 5th element[1] of the periodic table, offers a stunning variety of bonding motifs.[2,3] This is due to the capability of boron to form different bonding types, ranging from fully delocalized structures as present in spherical[4] and planar[5–7] antiaromatic species to multicenter, and two-center bonds.[8] Due to its electron deficiency, boron can form very stable anionic clusters, including those discussed in this article. Bonding motifs include planar structures,[5,6,9–12] some of them exhibiting high structural fluxionality,[12–17] dense 2D[18,19] and 3D materials[20] and more exotic ones such as all-boron fullerenes.[21] Arranged in wheels with strong two-center two-electron σ bonds around a central atom or a planar cluster, boron can stabilize metals[22] with a coordination number of 10 in two dimensions.[23,24] Cluster chemistry enables detailed gas phase studies of the chemistry of boron in close collaboration between experiment and high-level theory.[25,26] The group of Alexander I. Boldyrev established highly precise predictive computational chemistry protocols[27,28] and electronic structure analysis tools[29,30] that

allowed for the characterization, interpretation and in-depth chemical analysis of numerous species that have been prepared in experiment.

Icosahedral boron clusters are intriguing systems of remarkable stability, yet they can also provide extremely high reactivity.[31] The core motif, an icosahedral cage composed of 12 symmetry-equivalent boron atoms, is surrounded by 12 hydrogens, halogens or other monovalent species (like cyano groups), to form perfectly symmetric, *closo*-dodecaborates ($[B_{12}X_{12}]^{2-}$ with X = H, halogen, CN) of I_h symmetry (Figure 1a). A particular feature of the B_{12} core is its extremely high electron affinity, which withdraws electron density even from halide ions, which become positively charged.[32]

The remarkable stability of the *closo*-dodecaborates leads to a range of applications: For example, $[B_{12}Cl_{12}]^{2-}$ is an extremely stable dianion commonly utilized in ionic liquids.[33,34] Also utilized for ionic liquids is $[B_{12}H_{11}R]^-$ (R = organic group).[35] Its stability makes it a promising agent for boron neutron capture therapy.[36,37] Further applications in surface and interface science are emerging since these anionic species can be deposited in self-organizing layers, as demonstrated for $[B_{12}Cl_{12}]^{2-}$.[38]

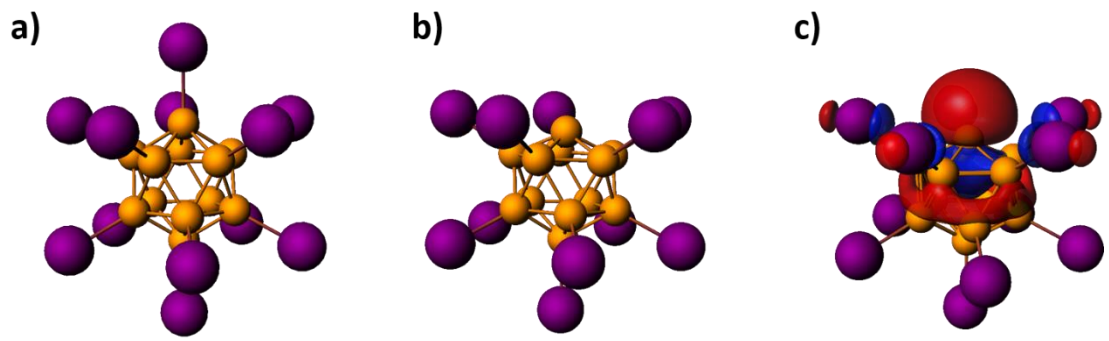

Figure 1. a) $[B_{12}I_{12}]^{2-}$ (I_h) cluster; b) $[B_{12}I_{11}]^{-}$ (C_{5v}) with a cavity that gives access to one boron atom; c) Visualization of the lowest unoccupied molecular orbital (LUMO) in $[B_{12}I_{11}]^{-}$ as isosurface at a value of 0.03 a.u. Color scheme for atoms: B: orange, I: purple.

As the icosahedral boron moiety dictates the properties of these intriguing clusters, it is interesting to access the constituting boron atoms directly. Indeed, it is possible to strip individual atoms off the periphery the B_{12} core (Figure 1b). This can be achieved by fragmentation in a mass spectrometer.[39,40] For $[B_{12}I_n]^{m-}$, (stable species in the ion trap are dianions (m = 2) with n = 12 to 9, anions (m = 1) with n = 11 to 1 and neutral B_{12} (n = 0, m = 0)), the fragmentation channel has been studied in detail[39] and individual species have been confirmed by infrared photodissociation (IRPD) spectroscopy.[41] The icosahedron remains intact after removal of the first five to six iodine ligands and transforms into a planar structure for x≤5,[42] finally yielding the planar neutral B_{12} cluster. A particularly interesting species is formed if only one iodide is removed: The $[B_{12}I_{11}]^{-}$ anion has a single accessible boron site (Figure 1b).

It is possible to form isostructural $[B_{12}X_{11}]^{-}$ clusters with other halogens, *i.e.* X = F, Cl, Br, I,[40] and also with X = CN.[43] The gas-phase reactivity of these molecular anions is demonstrated by the remarkably strong interaction with noble gas (Ng) atoms. Some $[B_{12}X_{11}Ng]^{-}$ complexes have already been studied experimentally and/or theoretically: $[B_{12}Cl_{11}]^{-}$ forms stable bonds with Xe

and Kr at room temperature, with binding energies (0 K) of respectively -108 and -81 kJ mol^{-1} as calculated at the MP2/6–311++G(2d,2p)/SDD level of theory.[44] The cyano cluster $[B_{12}(CN)_{11}]^-$ binds Ar[43] as well as Ne.[45] The $[B_{12}(CN)_{11}Ne]^-$ complex is experimentally stable up to 50 K, and the Ne attachment enthalpy at 0 K was calculated to be -9 kJ mol^{-1}, employing the B3LYP-D3(BJ)/def2-QZVPP level of theory.[45] The larger Ar binds significantly more strongly with -61±5 kJ mol^{-1} at 0 K (CCSD(T)/cc-pVTZ//MP2/cc-pVTZ) and is found to be stable at room temperature.[43]

Here we present a systematic theoretical investigation on the binding of the noble gases He, Ne, Ar, Kr, and Xe to the series of $[B_{12}X_{11}]^-$ molecular anions, with X = F, Cl, Br, I and CN. We will discuss the trends in the Gibbs energy of complexation reaction (following the reaction $[B_{12}X_{11}]^-$ +Ng → $[B_{12}X_{11}Ng]^-$, in the following referred to as *Gibbs energy*) and the structural features of the noble gas–containing complexes $[B_{12}X_{11}Ng]^-$ by comparing the predictions as obtained for the various X and Ng substituents. We will show some surprising trends: While for all X the Gibbs energy increases in magnitude with the size of the Ng atom, the affinity of the individual $[B_{12}X_{11}]^-$ species towards the noble gas atoms changes with the halogen. Notably, our calculations suggest, that all combinations of X with the heavy noble gases Ar, Kr and Xe form stable bonds up to room temperature. Furthermore, at 0 K also all combinations of X with Ne and the combination of $[B_{12}Cl_{11}]^-$ and $[B_{12}I_{11}]^-$ with He form stable bonds, while the He and Ne complexes become unstable at higher temperature. The charge transfer from the Ng atom to the $[B_{12}X_{11}]^-$ moiety is remarkably large, reaching 1/3 electronic charge in the case of the $[B_{12}(CN)_{11}Xe]^-$ complex.

METHODS Full geometry optimizations and vibrational analyses (within the harmonic approximation) have been carried out employing density-functional theory (DFT) at the hybrid PBE0[46,47] functional level and the Slater-type TZP[48] basis set. We used the zero order regular

approximation (ZORA)[49] to correct for scalar-relativistic effects and empirically corrected for London dispersion with Grimme's D3 scheme[50] together with Becke-Johnson (BJ) damping.[51] All DFT calculations have been carried out using the Amsterdam Modelling Suite (AMS) with the Amsterdam Density Functional (ADF) 2016 code [52–54] For the thermochemical calculations, the ideal gas approximation was used. Partial atomic charges have been calculated by performing QTAIM (Bader) analysis.[55] To substantiate the DFT energies, we performed single-point calculations on the optimized DFT geometries using the DLPNO-CCSD(T)[56,57] method with the def2-TZVPP[58] basis set and def2-TZVPP/C auxiliary basis[59] and NormalPNO cutoff thresholds[60] as implemented in the ORCA code.[61] To improve the stability of the calculations, very tight SCF convergence criteria and slow convergence were used for the reference HF calculations. The difference between both methods is shown in Figure S1, which shows lower binding energies for the PBE0-D3(BJ) calculations compared to the higher-level coupled cluster approximation. While the differences are within the expected accuracy range of 5 kJ mol^{-1} for He and Ne complexes, it appears as though PBE0-D3(BJ) underestimates the complexation energy by about 10-20 %. However, the general trends reported here are the same at both the DFT and the DLPNO-CCSD(T) levels of theory. For accuracy reasons, however, we report all energies at the DLPNO-CCSD(T) levels of theory, while geometries and frequencies, and related entropy, are calculated with DFT. Enthalpy $H = U + pV$ with the zero-point energy (ZPE) corrected internal energy U and the Gibbs energy $G = H - TS$ were calculated within the ideal gas approximation $pV = nRT$ and the harmonic approximation for the frequencies entering the ZPE and entropy terms. The vibrational frequencies were scaled by a factor of 0.9944.[62] The same settings have been used for the calculation of infrered spectra, which are, for visualization, convoluted by a Lorentzian of 7 cm^{-1} width.

RESULTS AND DISCUSSION The particularly strong activity of the $[B_{12}X_{11}]^-$ anions is reflected in the strongly localized form of their lowest unoccupied molecular orbital (LUMO) centered at the bare boron atom, as exemplarily shown for $[B_{12}I_{11}]^-$ in Figure 1c.

Figure 2a and Table S1 give the enthalpies ΔH of the complexation reaction $[B_{12}X_{11}]^- + Ng \rightarrow [B_{12}X_{11}Ng]^-$ at 0 K based on DLPNO-CCSD(T)//DFT (see Methods) Born-Oppenheimer energies and zero-point energies obtained via the harmonic approximation. Based on these results, we can distinguish two groups of $[B_{12}X_{11}Ng]^-$ complexes: Those with the light-weight He and Ne, and those with the heavier Ar, Kr and Xe. The light-weight Ngs show very weak, if any, attraction and both He and Ne would desorb at room temperature for all complexes studied here (Figure 2b, Table S2). While all $[B_{12}X_{11}Ne]^-$ species are predicted to be marginally stable at 0 K, only the chlorinated and iodinated derivatives attract He at 0 K with interaction energies of about 1 kJ mol^{-1}. The weak interaction of He and Ne can be anticipated in light of the low polarizability of both atoms (Table 1) and is reflected in the negligible charge transfer from the boron cluster to the Ng atoms (Figure 2c, Table S3).

In contrast, a roughly linear increase of the interaction energy with increasing the size of Ng is predicted for all $[B_{12}X_{11}Ng]^-$ adducts with Ar, Kr and Xe, with ΔH(T=0K) almost reaching -140 kJ mol^{-1} for the $[B_{12}(CN)_{11}Xe]^-$ complex (Figure 2a, Table S1). Thermal effects are significant: they weaken the interaction for all complexes by about 40 kJ mol^{-1} at room temperature compared to 0 K. When going down the group of noble gases in the periodic table, the interaction strengthens by about 25 kJ mol^{-1} per shell (see Figure 2b, Table S2). This again nearly linear relationship is expected from the Ng polarizabilities, and is accompanied by a significant electron transfer from the noble gas to the anionic boron cluster (see Bader charges in Figure 2c, Table S3). Among the

clusters with halogen atoms, those with Cl and Br show the strongest interaction, while those with I and F show slightly weaker interactions. There is no correlation with either the size, or the electron affinity of the halogens. The cyano-substituted dodecaborates bind Ngs significantly more strongly compared to the halogenated $[B_{12}X_{11}]^-$ anions. Qualitatively, all $[B_{12}X_{11}Ng]^-$ adducts with Ng = Ar, Kr, Xe are predicted to be stable at room temperature.

Table 1. Characteristic values for noble gases and halogens. For noble gases Ng, the atomic volume V and polarizability α are given. For halogens X the ionic radius R of X^- and the electron affinity EA are given. All data is taken from the literature.

Ng	**V (Å^3)**	**α (Å^3)**[63]		**X**	**R (Å)**[64]	**EA (eV)**
He	12	0.21		F	0.71	3.401[65,66]
Ne	15	0.4		Cl	0.99	3.613[67]
Ar	23	1.64		Br	1.14	3.364[65]
Kr	35	2.48		I	1.33	3.059[68,69]
Xe	42	4.04				

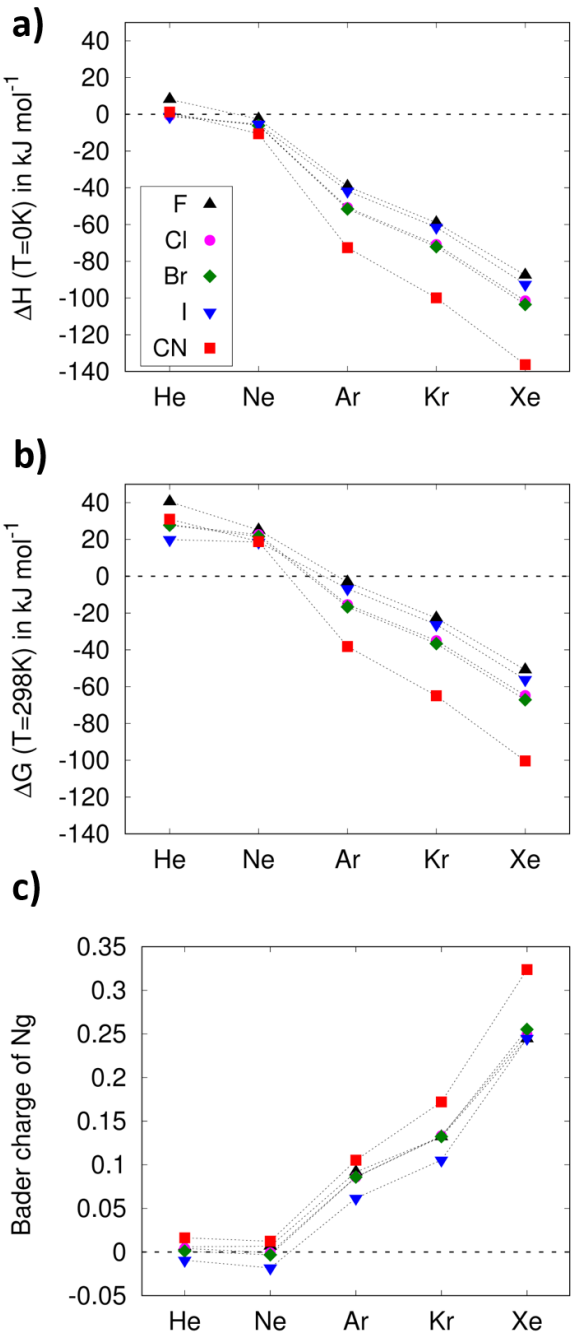

Figure 2: a) Enthalpy Δ*H* at 0 K and b) Gibbs energy Δ*G* at 298.15 K of the complexation reaction $[B_{12}X_{11}]^- + Ng \rightarrow [B_{12}X_{11}Ng]^-$ (X = F, Cl, Br, I and CN, and Ng = He to Xe). Calculations at the DLPNO-CCSD(T)/def2-TZVPP//PBE0-D3(BJ)/ZORA scalar/TZP level of theory (resp. values are listed in Tables S1 and S2). c) Bader charge of the Ng atom within $[B_{12}X_{11}Ng]^-$, as calculated at the PBE0-D3(BJ)/ZORA scalar/TZP level of theory. Lines are guides to the eye.

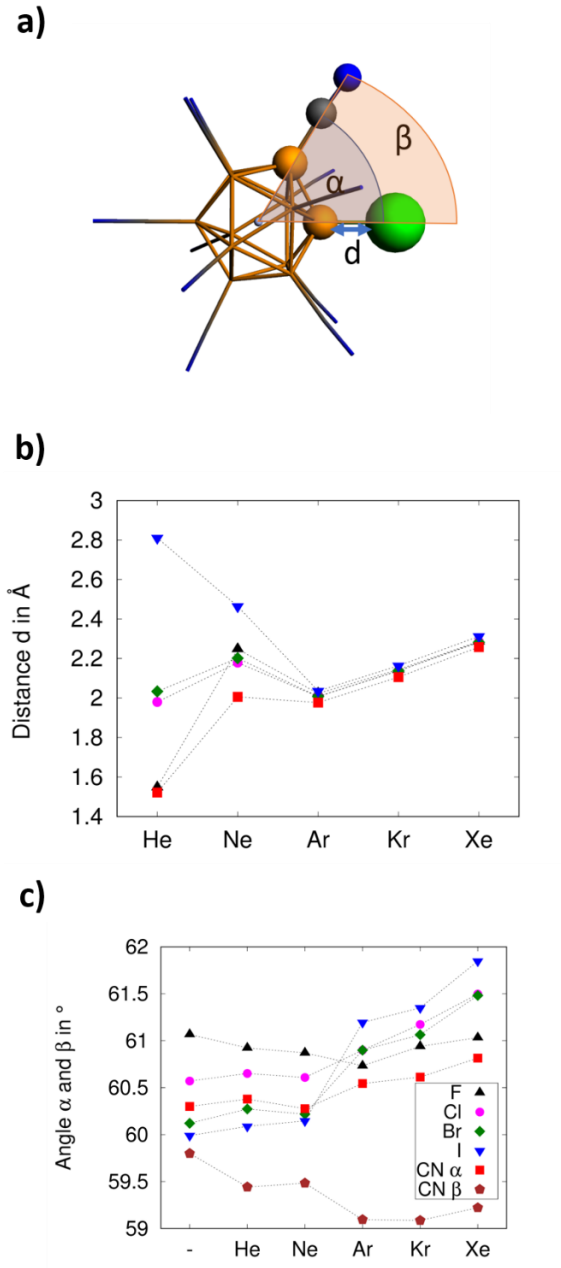

Figure 1: a) Combined ball-and-stick representation of a $[B_{12}(CN)_{11}Ng]^-$ adduct, illustrating the B–Ng distance, *d*, and the definition of the Ng-B_{12}-X angles α and β characterizing the size of the cavity in $[B_{12}X_{11}]^-$ prone to attack from an Ng atom. Color legend: B orange, Ng atom green, N blue, C grey. b) B–Ng equilibrium distance *d* (in Å)) and c) Ng-B_{12}-X angles between the Ng atom, the center of the B_{12} cage, and the adjacent X ligand (in °)) as predicted for $[B_{12}X_{11}Ng]^-$ (X = F to I and CN, and Ng = He to Xe) at the PBE0-D3(BJ)/ZORA scalar/TZP level of theory.

Figure 3b) shows the equilibrium distance between the Ng and the adjacent boron atom. Again, a strong difference is seen between light-weight He and Ne and the heavier Ng atoms. For the former, no particular trend is observed, because the minimal interaction results in very shallow potential energy surfaces without a pronounced minimum. For the heavier atoms, the calculated B–Ng equilibrium distances are about 0.10 to 0.25 Å longer than the sum of the covalent radii of the two corresponding atoms. The B–Ng equilibrium distance (for Ng = Ar, Kr and Xe) differs by only 0.13 to 0.15 Å within the series of X ligands, with X = CN marking the shortest and X = I the longest equilibrium distance. The most pronounced difference in the vibrational frequency of the B–Ng stretching mode, ν_{B-Ng}, in $[B_{12}X_{11}Ng]^-$ is predicted for the adducts with the heavier Ar, Kr and Xe as compared to those with the lighter He and Ne. While for the halogenated species, this difference is in the order of 17±5 cm^{-1}, it reaches 40 cm^{-1} for the cyano adducts of Ar and Ne. In all Ng-containing complexes with a given halogen ligand, ν_{B-Ng} differs by only 1 to 7 cm^{-1} when Ng = Ar, Kr and Xe, and is essentially the same for the two light-weight Ngs (Table S6). The cavity formed by the missing X atom closes slightly, as indicated 40 cm^{-1} when comparing the cyano by the angles shown in Figure 3b (for definition see 3a). In a perfect icosahedron, the angle, α, between the center of the $[B_{12}X_{12}]^{2-}$ cage and two adjacent X ligands is 63.4°. Upon removal of one X ligand, α decrease to only 60.5° (almost independently on X). The cavity size is influenced by the size of the Ng atom. For X = F, the cavity shrinks even further, by adding the Ng. Whereas the angle increases for the other systems, although it still remains smaller compared to the $[B_{12}X_{12}]^{2-}$ cluster. The CN ligands are special in this case, as they can also bend the B–C–N angle to better enclose the Ng atom. This shows in rather small N-center-Ng angles of ~59° (Fig. 3a/c).

SUMMARY We systematically explored the complexation of the molecular anions $[B_{12}X_{11}]^-$ (X = F, Cl, Br, I and CN) with the noble gas atoms from He to Xe. While light-weight He and Ne show negligible interaction with $[B_{12}X_{11}]^-$ and the corresponding $[B_{12}X_{11}Ng]^-$ adducts are unstable at room temperature, the heavier Ng atoms form stable complexes with Gibbs energies of attachment reaching -100 kJ mol^{-1} at 298 K, which is significantly higher than the energy of typical van der Waals complexes. Although the Ng atoms are bound to an anionic cluster we observe significant electron transfer away from the bound Ng indicating the unusually strong electron affinity of the $[B_{12}X_{11}]^-$ species. The cavity created by the missing X ligand is occupied by the Ng atom, and a small structural distortion of the icosahedral symmetry is present in all studied clusters. The presence of a bare boron atom with electrophilic character triggers the remarkable chemical activity of $[B_{12}X_{11}]^-$ (X = halogen or cyano group), as demonstrated by the strong affinity of these clusters to Kr, Ar and Xe despite their anionic nature.

AUTHOR INFORMATION

Corresponding Author

*thomas.heine@tu-dresden.de

Author Contributions

KW carried out all calculations and prepared a first version of the manuscript. The data was discussed jointly and all authors contributed in revising the manuscript. All authors have given approval to the final version of the manuscript.

Funding Sources

KW and TW thank the European Social Fund for a PhD fellowship. We thank ZIH Dresden for computational resources.

REFERENCES

References

(1) Hnyk, D.; McKee, M., Eds. *Boron*:*The Fifth Element*, 1st ed. 2015; Challenges and Advances in Computational Chemistry and Physics, Vol. 20; Springer International Publishing, 2015. DOI: 10.1007/978-3-319-22282-0.

(2) Fox, M. A.; Wade, K. Evolving patterns in boron cluster chemistry. *Pure and Applied Chemistry* **2003**, *75* (9), 1315–1323. DOI: 10.1351/pac200375091315.

(3) Gribanova, T. N.; Minyaev, R. M.; Minkin, V. I.; Boldyrev, A. I. Novel architectures of boron. *Struct Chem* **2020**, *31* (6), 2105–2128. DOI: 10.1007/s11224-020-01606-9.

(4) King, R. B.; Heine, T.; Corminboeuf, C.; Schleyer, P. v. R. Antiaromaticity in bare deltahedral silicon clusters satisfying Wade's and Hirsch's rules: an apparent correlation of antiaromaticity with high symmetry. *Journal of the American Chemical Society* **2004**, *126* (2), 430–431. DOI: 10.1021/ja036259.

(5) Huang, W.; Sergeeva, A. P.; Zhai, H.-J.; Averkiev, B. B.; Wang, L.-S.; Boldyrev, A. I. A concentric planar doubly π-aromatic B_{19}^- cluster. *Nat Chem* **2010**, *2* (3), 202–206. DOI: 10.1038/NCHEM.534. Published Online: Jan. 24, 2010.

(6) Sergeeva, A. P.; Averkiev, B. B.; Zhai, H.-J.; Boldyrev, A. I.; Wang, L.-S. All-boron analogues of aromatic hydrocarbons: B17- and B18-. *The Journal of Chemical Physics* **2011**, *134* (22), 224304. DOI: 10.1063/1.3599452.

(7) Alexandrova, A. N.; Boldyrev, A. I.; Zhai, H.-J.; Wang, L.-S.; Steiner, E.; Fowler, P. W. Structure and Bonding in B 6- and B 6 : Planarity and Antiaromaticity. *Journal of Physical Chemistry A* **2003**, *107* (9), 1359–1369. DOI: 10.1021/jp0268866.

(8) Alexandrova, A. N.; Boldyrev, A. I.; Zhai, H.-J.; Wang, L.-S. All-boron aromatic clusters as potential new inorganic ligands and building blocks in chemistry. *Coordination Chemistry Reviews* **2006**, *250* (21-22), 2811–2866. DOI: 10.1016/j.ccr.2006.03.032.

(9) Zhai, H.-J.; Alexandrova, A. N.; Birch, K. A.; Boldyrev, A. I.; Wang, L.-S. Hepta- and octacoordinate boron in molecular wheels of eight- and nine-atom boron clusters: observation and confirmation. *Angewandte Chemie-International Edition* **2003**, *42* (48), 6004–6008. DOI: 10.1002/anie.200351874.

(10) Popov, I. A.; Piazza, Z. A.; Li, W. L.; Wang, L. S.; Boldyrev, A. I. A combined photoelectron spectroscopy and ab initio study of the quasi-planar B-24(-) cluster. *J. Chem. Phys.* **2013**, *139* (14). DOI: 10.1063/1.4824156.

(11) Sergeeva, A. P.; Piazza, Z. A.; Romanescu, C.; Li, W.-L.; Boldyrev, A. I.; Wang, L.-S. B22- and B23-: all-boron analogues of anthracene and phenanthrene. *Journal of the American Chemical Society* **2012**, *134* (43), 18065–18073. DOI: 10.1021/ja307605t. Published Online: Oct. 17, 2012.

(12) Martinez-Guajardo, G.; Sergeeva, A. P.; Boldyrev, A. I.; Heine, T.; Ugalde, J. M.; Merino, G. Unravelling phenomenon of internal rotation in B_{13}^+ through chemical bonding analysis. *Chemical Communications* **2011**, *47* (22), 6242–6244. DOI: 10.1039/C1CC10821B.

(13) Sergeeva, A. P.; Popov, I. A.; Piazza, Z. A.; Li, W.-L.; Romanescu, C.; Wang, L.-S.; Boldyrev, A. I. Understanding boron through size-selected clusters: structure, chemical bonding, and fluxionality.

Accounts of chemical research **2014**, *47* (4), 1349–1358. DOI: 10.1021/ar400310g. Published Online: Mar. 24, 2014.
(14) Cervantes-Navarro, F.; Martinez-Guajardo, G.; Osorio, E.; Moreno, D.; Tiznado, W.; Islas, R.; Donald, K. J.; Merino, G. Stop rotating!:One substitution halts the B-19(-) motor. *Chemical Communications* **2014**, *50* (73), 10680–10682. DOI: 10.1039/c4cc03698k.
(15) Jalife, S.; Liu, L.; Pan, S.; Cabellos, J. L.; Osorio, E.; Lu, C.; Heine, T.; Donald, K. J.; Merino, G. Dynamical behavior of boron clusters. *Nanoscale* **2016**, *8* (40), 17639–17644. DOI: 10.1039/c6nr06383g.
(16) Jiménez-Halla, J. Oscar C; Islas, R.; Heine, T.; Merino, G. B_{19}^-:An Aromatic Wankel Motor. *Angewandte Chemie International Edition* **2010**, *49* (33), 5668–5671. DOI: 10.1002/anie.201001275.
(17) Merino, G.; Heine, T. And Yet It Rotates:The Starter for a Molecular Wankel Motor. *Angewandte Chemie-International Edition* **2012**, *51* (41), 10226–10227. DOI: 10.1002/anie.201206188.
(18) Zhou, X.-F.; Oganov, A. R.; Wang, Z.; Popov, I. A.; Boldyrev, A. I.; Wang, H.-T. Two-dimensional magnetic boron. *Phys. Rev. B* **2016**, *93* (8).
(19) Yang, L.-M.; Bačić, V.; Popov, I. A.; Boldyrev, A. I.; Heine, T.; Frauenheim, T.; Ganz, E. Two-dimensional Cu2Si monolayer with planar hexacoordinate copper and silicon bonding. *Journal of the American Chemical Society* **2015**, *137* (7), 2757–2762. DOI: 10.1021/ja513209c. Published Online: Feb. 13, 2015.
(20) Olson, J. K.; Boldyrev, A. I. Planar to 3D Transition in the B6Hy Anions. *Journal of Physical Chemistry A* **2013**, *117* (7), 1614–1620.
(21) Zhai, H.-J.; Zhao, Y.-F.; Li, W.-L.; Chen, Q.; Bai, H.; Hu, H.-S.; Piazza, Z. A.; Tian, W.-J.; Lu, H.-G.; Wu, Y.-B.; Mu, Y.-W.; Wei, G.-F.; Liu, Z.-P.; Li, J.; Li, S.-D.; Wang, L.-S. Observation of an all-boron fullerene. *Nat Chem* **2014**, *6* (8), 727–731. DOI: 10.1038/NCHEM.1999. Published Online: Jul. 13, 2014.
(22) Romanescu, C.; Galeev, T. R.; Li, W.-L.; Boldyrev, A. I.; Wang, L.-S. Aromatic metal-centered monocyclic boron rings: Co©B8- and Ru©B9-. *Angewandte Chemie International Edition* **2011**, *50* (40), 9334–9337. DOI: 10.1002/anie.201104166. Published Online: Aug. 31, 2011.
(23) Galeev, T. R.; Romanescu, C.; Li, W.-L.; Wang, L.-S.; Boldyrev, A. I. Observation of the highest coordination number in planar species: decacoordinated Ta©B10(-) and Nb©B10(-) anions. *Angewandte Chemie International Edition* **2012**, *51* (9), 2101–2105. DOI: 10.1002/anie.201107880.
(24) Heine, T.; Merino, G. What is the maximum coordination number in a planar structure? *Angewandte Chemie International Edition* **2012**, *51* (18), 4275–4276. DOI: 10.1002/anie.201201166.
(25) Jian, T.; Chen, X.; Li, S.-D.; Boldyrev, A. I.; Li, J.; Wang, L.-S. Probing the structures and bonding of size-selected boron and doped-boron clusters. *Chemical Society reviews* **2019**, *48* (13), 3550–3591. DOI: 10.1039/c9cs00233b.
(26) Pan, S.; Barroso, J.; Jalife, S.; Heine, T.; Asmis, K. R.; Merino, G. Fluxional Boron Clusters: From Theory to Reality. *Accounts of chemical research* **2019**, *52* (9), 2732–2744. DOI: 10.1021/acs.accounts.9b00336. Published Online: Sep. 5, 2019.
(27) Sergeeva, A. P.; Zubarev, D. Y.; Zhai, H.-J.; Boldyrev, A. I.; Wang, L.-S. A photoelectron spectroscopic and theoretical study of B16- and B16(2-): an all-boron naphthalene. *Journal of the American Chemical Society* **2008**, *130* (23), 7244–7246. DOI: 10.1021/ja802494z. Published Online: May. 15, 2008.
(28) Zhai, H.-J.; Wang, L.-S.; Alexandrova, A. N.; Boldyrev, A. I. Electronic structure and chemical bonding of B5− and B5 by photoelectron spectroscopy and ab initio calculations. *J. Chem. Phys.* **2002**, *117* (17), 7917–7924. DOI: 10.1063/1.1511184.

(29) Zubarev, D. Y.; Boldyrev, A. I. Developing paradigms of chemical bonding: adaptive natural density partitioning. *Physical chemistry chemical physics : PCCP* **2008**, *10* (34), 5207–5217. DOI: 10.1039/b804083d. Published Online: Jul. 3, 2008.
(30) Zubarev, D. Y.; Boldyrev, A. I. Comprehensive analysis of chemical bonding in boron clusters. *J. Comput. Chem.* **2007**, *28* (1), 251–268. DOI: 10.1002/jcc.20518.
(31) Bolli, C.; Derendorf, J.; Keßler, M.; Knapp, C.; Scherer, H.; Schulz, C.; Warneke, J. Synthesis, Crystal Structure, and Reactivity of the Strong Methylating Agent Me2B12Cl12. *Angewandte Chemie International Edition* **2010**, *49* (20), 3536–3538. DOI: 10.1002/anie.200906627.
(32) Zeonjuk, L. L.; Vankova, N.; Knapp, C.; Gabel, D.; Heine, T. On the gas-phase dimerization of negatively charged closo-dodecaborates: a theoretical study. *Physical chemistry chemical physics : PCCP* **2013**, *15* (25), 10358–10366. DOI: 10.1039/C3CP50722J. Published Online: May. 15, 2013.
(33) Geis, V.; Guttsche, K.; Knapp, C.; Scherer, H.; Uzun, R. Synthesis and characterization of synthetically useful salts of the weakly-coordinating dianion $[B_{12}Cl_{12}]^{2-}$. *Dalton Transactions* **2009** (15), 2687–2694. DOI: 10.1039/B821030F.
(34) Nieuwenhuyzen, M.; Seddon, K. R.; Teixidor, F.; Puga, A. V.; Viñas, C. Ionic Liquids Containing Boron Cluster Anions. *Inorganic Chemistry* **2009**, *48* (3), 889–901. DOI: 10.1021/ic801448w.
(35) Justus, E.; Rischka, K.; Wishart, J. F.; Werner, K.; Gabel, D. Trialkylammoniododecaborates: anions for ionic liquids with potassium, lithium and protons as cations. *Chemistry (Weinheim an der Bergstrasse, Germany)* **2008**, *14* (6), 1918–1923. DOI: 10.1002/chem.200701427.
(36) Dymova, M. A.; Taskaev, S. Y.; Richter, V. A.; Kuligina, E. V. Boron neutron capture therapy: Current status and future perspectives. *Cancer communications (London, England)* **2020**, *40* (9), 406–421. DOI: 10.1002/cac2.12089. Published Online: Aug. 17, 2020.
(37) Barth, R. F.; Coderre, J. A.; Vicente, M. G. H.; Blue, T. E. Boron neutron capture therapy of cancer:Current status and future prospects. *Clinical Cancer Research* **2005**, *11* (11), 3987–4002. DOI: 10.1158/1078-0432.ccr-05-0035.
(38) Warneke, J.; McBriarty, M. E.; Riechers, S. L.; China, S.; Engelhard, M. H.; Aprà, E.; Young, R. P.; Washton, N. M.; Jenne, C.; Johnson, G. E.; Laskin, J. Self-organizing layers from complex molecular anions. *Nature Communications* **2018**, *9* (1), 1889. DOI: 10.1038/s41467-018-04228-2. Published Online: May. 14, 2018.
(39) Farràs, P.; Vankova, N.; Zeonjuk, L. L.; Warneke, J.; Dülcks, T.; Heine, T.; Viñas, C.; Teixidor, F.; Gabel, D. From an Icosahedron to a Plane:Flattening Dodecaiodo-dodecaborate by Successive Stripping of Iodine. *Chemistry – A European Journal* **2012**, *18* (41), 13208–13212. DOI: 10.1002/chem.201200828.
(40) Warneke, J.; Dülcks, T.; Knapp, C.; Gabel, D. Collision-induced gas-phase reactions of perhalogenated closo-dodecaborate clusters--a comparative study. *Physical chemistry chemical physics : PCCP* **2011**, *13* (13), 5712–5721. DOI: 10.1039/C0CP02386H. Published Online: Feb. 10, 2011.
(41) Fagiani, M. R.; Zeonjuk, L. L.; Esser, T. K.; Gabel, D.; Heine, T.; Asmis, K. R.; Warneke, J. Opening of an icosahedral boron framework:A combined infrared spectroscopic and computational study. *Chemical Physics Letters* **2015**, *625*, 48–52.
(42) Gong, L.-F.; Li, W.; Osorio, E.; Wu, X.-M.; Heine, T.; Liu, L. The effects of halogen elements on the opening of an icosahedral B12 framework. *The Journal of Chemical Physics* **2017**, *147* (14), 144302. DOI: 10.1063/1.4998948.
(43) Mayer, M.; van Lessen, V.; Rohdenburg, M.; Hou, G.-L.; Yang, Z.; Exner, R. M.; Aprà, E.; Azov, V. A.; Grabowsky, S.; Xantheas, S. S.; Asmis, K. R.; Wang, X.-B.; Jenne, C.; Warneke, J. Rational design of an argon-binding superelectrophilic anion. *Proceedings of the National Academy of Sciences of the United*

States of America **2019**, *116* (17), 8167–8172. DOI: 10.1073/pnas.1820812116. Published Online: Apr. 5, 2019.
(44) Rohdenburg, M.; Mayer, M.; Grellmann, M.; Jenne, C.; Borrmann, T.; Kleemiss, F.; Azov, V. A.; Asmis, K. R.; Grabowsky, S.; Warneke, J. Superelectrophilic Behavior of an Anion Demonstrated by the Spontaneous Binding of Noble Gases to B12 Cl11 <sup. *Angewandte Chemie International Edition* **2017**, *56* (27), 7980–7985. DOI: 10.1002/anie.201702237. Published Online: May. 31, 2017.
(45) Mayer, M.; Rohdenburg, M.; van Lessen, V.; Nierstenhöfer, M. C.; Aprà, E.; Grabowsky, S.; Asmis, K. R.; Jenne, C.; Warneke, J. First steps towards a stable neon compound: observation and bonding analysis of B12(CN)11Ne. *Chemical communications (Cambridge, England)* **2020**, *56* (33), 4591–4594. DOI: 10.1039/D0CC01423K. Published Online: Mar. 24, 2020.
(46) Adamo, C.; Barone, V. Toward reliable density functional methods without adjustable parameters: The PBE0 model. *J. Chem. Phys.* **1999**, *110* (13), 6158–6170. DOI: 10.1063/1.478522.
(47) Ernzerhof, M.; Scuseria, G. E. Assessment of the Perdew–Burke–Ernzerhof exchange-correlation functional. *J. Chem. Phys.* **1999**, *110* (11), 5029–5036. DOI: 10.1063/1.478401.
(48) van Lenthe, E.; Baerends, E. J. Optimized Slater-type basis sets for the elements 1-118. *Journal of Computational Chemistry* **2003**, *24* (9), 1142–1156. DOI: 10.1002/jcc.10255.
(49) van Lenthe, E.; Ehlers, A.; Baerends, E.-J. Geometry optimizations in the zero order regular approximation for relativistic effects. *J. Chem. Phys.* **1999**, *110* (18), 8943–8953. DOI: 10.1063/1.478813.
(50) Grimme, S.; Antony, J.; Ehrlich, S.; Krieg, H. A consistent and accurate ab initio parametrization of density functional dispersion correction (DFT-D) for the 94 elements H-Pu. *The Journal of Chemical Physics* **2010**, *132* (15), 154104. DOI: 10.1063/1.3382344.
(51) Grimme, S.; Ehrlich, S.; Goerigk, L. Effect of the damping function in dispersion corrected density functional theory. *J. Comput. Chem.* **2011**, *32* (7), 1456–1465. DOI: 10.1002/jcc.21759. Published Online: Mar. 1, 2011.
(52) te Velde, G.; Bickelhaupt, F. M.; Baerends, E. J.; Fonseca Guerra, C.; van Gisbergen, S. J. A.; Snijders, J. G.; Ziegler, T. Chemistry with ADF. *J. Comput. Chem.* **2001**, *22* (9), 931–967. DOI: 10.1002/jcc.1056.
(53) AMS 2019, SCM, Theoretical Chemistry, Vrije Universiteit, Amsterdam, The Netherlands, http://www.scm.com.
(54) Fonseca Guerra, C.; Snijders, J. G.; te Velde, G.; Baerends, E. J. Towards an order- N DFT method. *Theoretical Chemistry Accounts: Theory, Computation, and Modeling (Theoretica Chimica Acta)* **1998**, *99* (6), 391–403. DOI: 10.1007/s002140050353.
(55) Tognetti, V.; Joubert, L. Density functional theory and Bader's atoms-in-molecules theory: towards a vivid dialogue. *Physical chemistry chemical physics : PCCP* **2014**, *16* (28), 14539–14550. DOI: 10.1039/C3CP55526G.
(56) Riplinger, C.; Sandhoefer, B.; Hansen, A.; Neese, F. Natural triple excitations in local coupled cluster calculations with pair natural orbitals. *The Journal of Chemical Physics* **2013**, *139* (13), 134101. DOI: 10.1063/1.4821834.
(57) Guo, Y.; Riplinger, C.; Becker, U.; Liakos, D. G.; Minenkov, Y.; Cavallo, L.; Neese, F. Communication: An improved linear scaling perturbative triples correction for the domain based local pair-natural orbital based singles and doubles coupled cluster method DLPNO-CCSD(T). *The Journal of Chemical Physics* **2018**, *148* (1), 11101. DOI: 10.1063/1.5011798.
(58) Weigend, F.; Ahlrichs, R. Balanced basis sets of split valence, triple zeta valence and quadruple zeta valence quality for H to Rn: Design and assessment of accuracy. *Physical chemistry chemical physics : PCCP* **2005**, *7* (18), 3297–3305. DOI: 10.1039/b508541a. Published Online: Aug. 4, 2005.

(59) Hellweg, A.; Hättig, C.; Höfener, S.; Klopper, W. Optimized accurate auxiliary basis sets for RI-MP2 and RI-CC2 calculations for the atoms Rb to Rn. *Theor Chem Acc* **2007**, *117* (4), 587–597. DOI: 10.1007/s00214-007-0250-5.
(60) Liakos, D. G.; Sparta, M.; Kesharwani, M. K.; Martin, J. M. L.; Neese, F. Exploring the Accuracy Limits of Local Pair Natural Orbital Coupled-Cluster Theory. *Journal of chemical theory and computation* **2015**, *11* (4), 1525–1539. DOI: 10.1021/ct501129s.
(61) Neese, F. The ORCA program system. *WIREs Comput Mol Sci* **2012**, *2* (1), 73–78. DOI: 10.1002/wcms.81.
(62) Kesharwani, M. K.; Brauer, B.; Martin, J. M. L. Frequency and zero-point vibrational energy scale factors for double-hybrid density functionals (and other selected methods): can anharmonic force fields be avoided? *The journal of physical chemistry. A* **2015**, *119* (9), 1701–1714. DOI: 10.1021/jp508422u. Published Online: Oct. 21, 2014.
(63) Campanell, F. C.; Battino, R.; Seybold, P. G. On the Role of Solute Polarizability in Determining the Solubilities of Gases in Liquids. *J. Chem. Eng. Data* **2010**, *55* (1), 37–40. DOI: 10.1021/je900558s.
(64) Shannon, R. D. Revised effective ionic radii and systematic studies of interatomic distances in halides and chalcogenides. *Acta Cryst A* **1976**, *32* (5), 751–767. DOI: 10.1107/S0567739476001551.
(65) Blondel; Cacciani; Delsart; Trainham. High-resolution determination of the electron affinity of fluorine and bromine using crossed ion and laser beams. *Physical review. A, General physics* **1989**, *40* (7), 3698–3701. DOI: 10.1103/PhysRevA.40.3698.
(66) Blondel, C.; Delsart, C.; Goldfarb, F. Electron spectrometry at the μeV level and the electron affinities of Si and F. *J. Phys. B: At. Mol. Opt. Phys.* **2001**, *34* (9), L281-L288. DOI: 10.1088/0953-4075/34/9/101.
(67) Berzinsh; Gustafsson; Hanstorp; Klinkmüller; Ljungblad; Mårtensson-Pendrill. Isotope shift in the electron affinity of chlorine. *Physical review. A, Atomic, molecular, and optical physics* **1995**, *51* (1), 231–238. DOI: 10.1103/PhysRevA.51.231.
(68) Peláez, R. J.; Blondel, C.; Delsart, C.; Drag, C. Pulsed photodetachment microscopy and the electron affinity of iodine. *J. Phys. B: At. Mol. Opt. Phys.* **2009**, *42* (12), 125001. DOI: 10.1088/0953-4075/42/12/125001.
(69) Rothe, S.; Sundberg, J.; Welander, J.; Chrysalidis, K.; Goodacre, T. D.; Fedosseev, V.; Fiotakis, S.; Forstner, O.; Heinke, R.; Johnston, K.; Kron, T.; Köster, U.; Liu, Y.; Marsh, B.; Ringvall-Moberg, A.; Rossel, R. E.; Seiffert, C.; Studer, D.; Wendt, K.; Hanstorp, D. Laser photodetachment of radioactive 128 I −. *J. Phys. G: Nucl. Part. Phys.* **2017**, *44* (10), 104003. DOI: 10.1088/1361-6471/aa80aa.
(70) Rohdenburg, M.; Mayer, M.; Grellmann, M.; Jenne, C.; Borrmann, T.; Kleemiss, F.; Azov, V. A.; Asmis, K. R.; Grabowsky, S.; Warneke, J. Superelektrophiles Verhalten eines Anions demonstriert durch spontane Bindung von Edelgasen an [B 12 Cl 11] −. *Angew. Chem.* **2017**, *129* (27), 8090–8096. DOI: 10.1002/ange.201702237.